

# Control of a Large Scale Solar Thermal Energy Storage System

Kody M. Powell, Thomas F. Edgar

**Abstract**—Dynamic simulation results for a thermal energy storage (TES) unit used in a parabolic trough concentrated solar power (CSP) system are presented. A two-tank-direct method is used for the thermal energy storage. The heat transfer fluid flow rate through the solar collector maintains a constant outlet temperature and the flow rate through the boiler regulates power output. The use of storage greatly improves the system's ability to provide power at a constant rate despite significant disturbances in the amount of solar radiation available. It can also shift times of power generation to better match times of consumer demand. By contrast, a CSP system without storage undergoes large fluctuations in power output, particularly during intermittent cloud cover. Adding a storage system increases the solar share of the power plant by over 80%, reducing the requirement for supplementary fossil energy by as much as 8.4 MWh daily.

## I. INTRODUCTION

THE intermittent nature of renewable energy resources, such as solar and wind, puts them at an inherent disadvantage when compared to fossil fuels. Fossil fuels essentially are stored energy, which can be dispatched on demand by combustion of the fuel. By contrast, solar and wind are available only when the sun is shining or the wind is blowing. In order to make these resources viable replacements for fossil fuels, economical energy storage technologies must be developed. Energy storage makes it possible to align energy production with consumer demand. Thermal energy storage (TES), or the storing of energy as heat or cooling, is a cost-effective technology with many potential applications [1].

Concentrating solar power (CSP) systems illustrate the value of TES technology. CSP systems concentrate solar radiation using mirrors or lenses to heat a fluid for a power plant or other application. Without storage, the power output from these systems is interrupted when a disturbance is introduced to the system. For example, when the sun goes behind a cloud, less energy is available, and the power output decreases accordingly.

Many advanced control techniques have been applied to concentrating solar power systems to overcome the problems caused by the sporadic nature of solar radiation. These techniques are generally focused on controlling the solar collector outlet temperature by varying the heat transfer fluid

(HTF) flow rate (the manipulated variable) through the collector field [2]. If no energy storage is considered, the power output from the plant will vary as solar radiation varies. Conversely, modeling the solar collector with a TES unit creates an additional manipulated variable: the flow rate from the storage tank to the load heat exchanger. Thus, while the collector field outlet temperature can still be controlled, the power delivered to the load can be controlled independently, making it possible to sustain constant power output during cloud cover, or to shift power output to better meet variable consumer demand.

Because the TES system represents only part of the overall energy system, dynamic modeling of the complete system is necessary to gain understanding of how the storage components interact with the other components of the system. In this paper, the focus of the simulation is on the TES system and how it is used to improve control of the power output.

## II. OVERVIEW OF THE SYSTEM

The thermal energy storage system modeled in this work uses the two-tank-direct configuration where the heat transfer fluid also acts as the energy storage medium. This requires two separate tanks, but eliminates the need for an additional heat exchanger to transfer heat from the collection HTF to the storage medium. The fluid is stored at its lower temperature in a cold tank, heated in the solar collector field, and then stored at an elevated temperature in the hot tank [3].

A parabolic trough solar collector field with east-west sun tracking is considered. The solar collector uses parabolic mirrors to concentrate direct solar radiation onto an absorber pipe, through which the HTF flows while it absorbs heat. A PID controller is used to control the outlet temperature using the mass flow rate ( $\dot{m}_1$ ) as the manipulated variable (see Figure 1).

The stored energy in the hot tank is delivered to the load by pumping the HTF through the solar boiler. In this model, it is assumed that saturated liquid water is fed to the boiler and it exits as saturated steam. In this exchange, the HTF returns to its lower temperature and is pumped back to the cold tank. The output power is represented by the flow rate of the saturated steam generated in the boiler. This flow rate is measured and a PID controller is used to control it with  $\dot{m}_2$  (the flow from the hot tank to the cold tank) used as a manipulated variable.

February 22, 2011.

Kody Merlin Powell, PhD Student, Department of Chemical Engineering, University of Texas at Austin, Austin, Texas, (email: powellk@che.utexas.edu)

Thomas Edgar, Professor, Department of Chemical Engineering, University of Texas at Austin, Austin, Texas, (email: tfedgar@austin.utexas.edu)

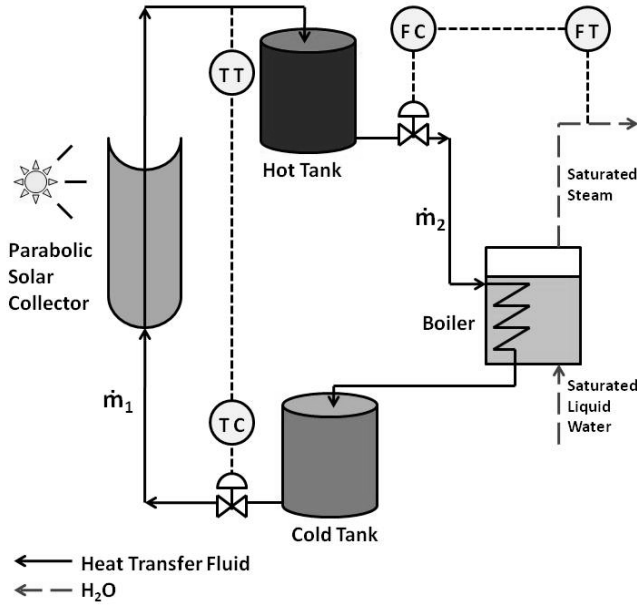


Figure 1: The two-tank-direct thermal energy storage system used with a parabolic trough solar collector field. The system uses the flow rate  $\dot{m}_1$  to control the fluid outlet temperature from the collector field and  $\dot{m}_2$  to control the steam flow rate from the boiler.

### III. MODEL FORMULATION

#### A. The Solar Collector

The solar collector consists of a parabolic-shaped mirror, which is used to focus solar radiation onto the absorber pipe. The absorber pipe is a long tube running down the focal point of the mirrors. It is enclosed in a glass envelope, which is mostly transparent to UV radiation, but opaque to IR radiation. The absorber pipe is designed to have a high absorptivity and a low emissivity, so that it absorbs high amounts of radiation, while minimizing radiative heat losses [4]. A cross-sectional view of the absorber pipe with glass envelope is shown below.

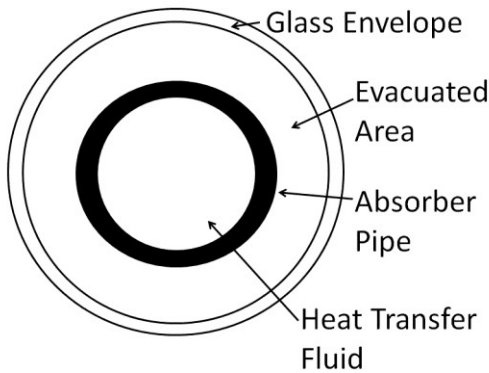


Figure 2: A cross-sectional view of the absorber pipe assembly.

Modeling of this system requires computing energy balances for the HTF, the absorber pipe, and the glass envelope. Neglecting radial temperature gradients and conductive heat transfer yields the following PDE, which represents the HTF energy balance:

$$\rho_F C_F A_{A,i} \frac{\partial T_F}{\partial t} = i \left[ \dots - h_p P_{A,i} (T_A - T_F) \right]$$

where  $\rho$  represents the density,  $C$ , the heat capacity,  $A$ , the cross-sectional area,  $T$ , the temperature,  $\dot{m}$ , the mass flow rate of the HTF,  $x$ , the axial distance along the collector,  $h_p$ , the convective heat transfer coefficient inside the pipe, and  $P$ , the perimeter. The subscript  $F$  refers to the heat transfer fluid,  $A$  to the absorber, and  $A,i$  to the inner dimensions of the absorber pipe.

The energy balance is also computed on the absorber pipe:

$$\rho_A C_A A_A \frac{\partial T_A}{\partial t} = h_p P_{A,i} (T_F - T_A) - \frac{\sigma}{\frac{1}{\varepsilon_A} + \frac{1 - \varepsilon_E}{\varepsilon_E} \left( \frac{r_{A,o}}{r_{E,i}} \right)} P_{A,o} (T_A^4 - T_E^4) + q_A'' w$$

where  $\varepsilon$  represents emissivity,  $\sigma$  is the Stefan-Boltzmann constant,  $q_A''$  is the radiative flux after accounting for optical inefficiencies (formula shown on page 3),  $r$  is the radius, and  $w$  is the solar collector width. The subscript  $A,o$  refers to the outer dimension of the absorber pipe,  $E$  refers to the glass envelope, and  $E,i$  refers to the inner dimension of the envelope. Convection between the absorber pipe and the glass envelope is neglected due to the vacuum between the two surfaces.

Similarly, the energy balance on the glass envelope is computed:

$$\rho_E C_E A_E \frac{\partial T_E}{\partial t} = \frac{\sigma}{\frac{1}{\varepsilon_A} + \frac{1 - \varepsilon_E}{\varepsilon_E} \left( \frac{r_{A,o}}{r_{E,i}} \right)} P_{A,i} (T_A^4 - T_E^4) - \sigma \varepsilon_E P_{E,o} (T_E^4 - T_{AIR}^4) - h_{AIR} P_{E,o} (T_E - T_{AIR})$$

where the subscript,  $AIR$ , refers to the ambient air properties.

Solutions to the three energy balance PDEs can be approximated by dividing the length of the collector into  $n$  discrete sections. This converts 3 PDEs into a set of  $3n$  ODEs. Derivatives are then approximated as follows:

$$\frac{dT}{dx} \approx \frac{T(i) - T(i-1)}{\Delta x}$$

The spatial discretization scheme is shown in Figure 3, where each cylindrical segment has a length of  $\Delta x$ . The system is solved in time using a Runge-Kutta (4,5) numerical integration to solve each segment with respect to time.

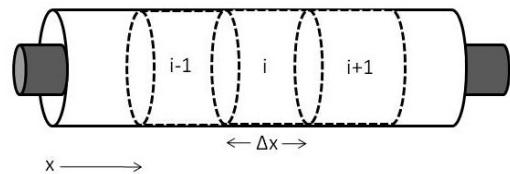


Figure 3: A side-view of the absorber pipe assembly illustrating discretization for numerical simulation.

### B. The Thermal Energy Storage Tanks

The TES tanks are modeled by dynamic mass and energy balances for mixed tanks. The mass balance for a tank is:

$$\rho_F \frac{dV}{dt} = \dot{i}$$

where  $V$  is the total volume of HTF in the tank and the subscripts *in* and *out* refer to flow in and out of the tank, respectively.

The energy balance for each tank is:

$$\rho_F C_F \frac{d(VT)}{dt} = C_F (T_{in} \dot{i} - T_{out} \dot{o} - T - T_{AIR})$$

where  $U$  is the overall heat transfer coefficient for the tank walls and  $A$  is the surface area of the tank subject to heat transfer. It is assumed that no heat transfer occurs from the top or bottom of either tank.

Because the volumes of HTF ( $V$ ) in the tanks are not constant, the energy balances are solved for the product  $VT$ , which is then divided by  $V$ , the solution to the mass balance to obtain the tank temperature,  $T$ .

In order to prevent the tanks from violating volume constraints, the following logic is included in the tank models:

If  $V_{Tank} = V_{High}$  and  $\dot{i}$

Then  $\dot{i} = 0$

If  $V = V_{Low}$  and  $\dot{o}$

Then  $\dot{o} = 0$

Initially, it is assumed that the cold tank is full of HTF at a low temperature and the hot tank is at its lower-limit volume at some elevated temperature, leading to the initial conditions:

$$V_{Hot}(t=0) = V_{Low}$$

$$V_{Cold}(t=0) = V_{High}$$

$$T_{Hot}(t=0) = T_{Hot,0}$$

$$T_{Cold}(t=0) = T_{Cold,0}$$

### C. The Boiler

The boiler model assumes the HTF enters a heating coil, which passes through a tank of saturated liquid water. The water side of the boiler is assumed to be at a constant temperature, while HTF inside the coil varies with time and distance along the coil. The energy balance on the HTF in the coil is as follows:

$$\rho_F C_F A_{p,i} \frac{\partial T_F}{\partial t} = \dot{i} - h_p P_{p,i} (T_B - T_F)$$

where  $z$  is the distance along the boiler coil and the subscripts  $p,i$  and  $B$  refer to the inner pipe and the boiler water temperature, respectively.

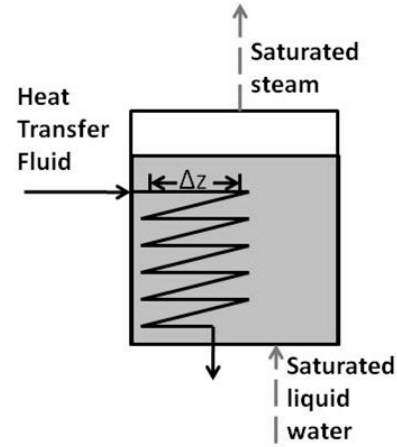


Figure 4: A diagram of the boiler showing the inner-pipe discretization for numerical simulation.

The saturated steam flow rate is then computed from a steady-state energy balance on the boiler:

$$\dot{i} = \dot{o} + \dot{m}_s h_{fg}$$

where  $h_{fg}$  refers to the enthalpy of vaporization of the water at  $T_B$ .

### D. Solar Irradiance

The ASHRAE model was used to predict solar beam irradiance as a function of the incidence angle on the collector surface. The equation for predicting the irradiance in the direction of rays ( $I_N$ ) is:

$$I_N = A \exp[-B / \cos(\theta_z)]$$

where  $A$  and  $B$  are constants based on the month of the year and  $\theta_z$  is the solar zenith angle [5]. The amount of radiation incident on the collector surface ( $I_C$ ) is given by:

$$I_C = I_N \cos(\theta)$$

where  $\theta$  is the incidence angle, which is a function of the location, the day of the year, and the time of day.

The incident radiation term is multiplied by the optical efficiency of the collector ( $\eta_{optical}$ ) and one minus the cloud factor ( $F_C$ ) to obtain the amount of solar flux absorbed by the absorber pipe ( $q_A$ ).

$$q_A = I_C \eta_{optical} (1 - F_C)$$

The optical efficiency is a function of  $v_A$  (the absorptivity of the absorber pipe),  $\tau_E$  (the envelope transmissivity),  $\alpha_M$  (the mirror reflectivity),  $\gamma$  (the intercept factor), and  $K$ , the incidence angle modifier [6].

$$\eta_{optical} = K v_A \tau_E \alpha_M \gamma$$

### E. Controllers

The collector field temperature control is done with a PID controller equipped with an anti-reset mechanism. For a system with storage, the power output is controlled using a PID controller, which is activated after the hot storage tank begins charging. The controllers are tuned using IMC tuning relations [7].

#### IV. SIMULATED CLOSED-LOOP RESULTS

##### A. Clear Day: System with No Storage

A parabolic trough steam generation plant designed to produce 1 MW thermal with a total collector area of 1,750 m<sup>2</sup> is considered. The control system is designed to control the collector outlet temperature at 650 K, with a boiler temperature of 450 K. Because there is no storage tank in this setup, the only manipulated variable is the HTF flow rate, which is the same through the collector field as it is through the boiler. The results of these simulations are shown in Figures 5-7. As Figure 7 indicates, a PID controller does an adequate job of keeping this temperature constant, aside from some initial overshoot. Keeping the collector outlet temperature constant, however, causes the HTF flow rate to vary, which results in a varying power output.

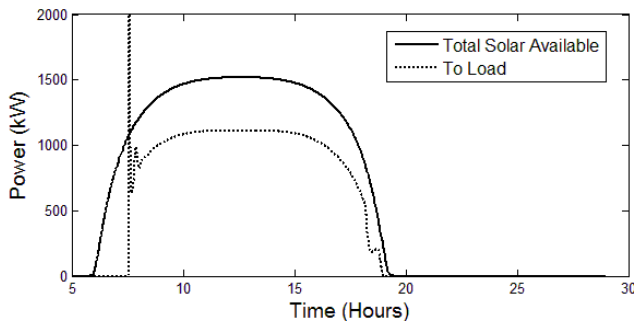


Figure 5: A plot of the total solar power available and the power delivered to the load for a parabolic trough collector system with no thermal storage.

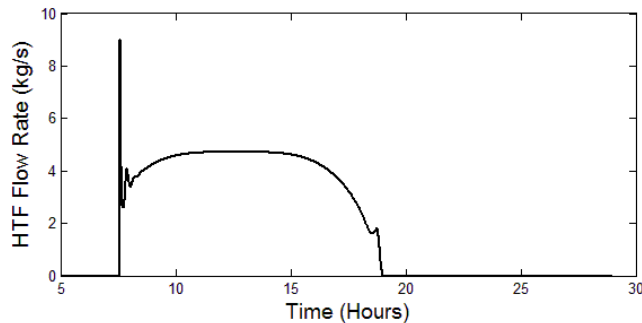


Figure 6: A plot of the HTF flow rate for a system with no storage.

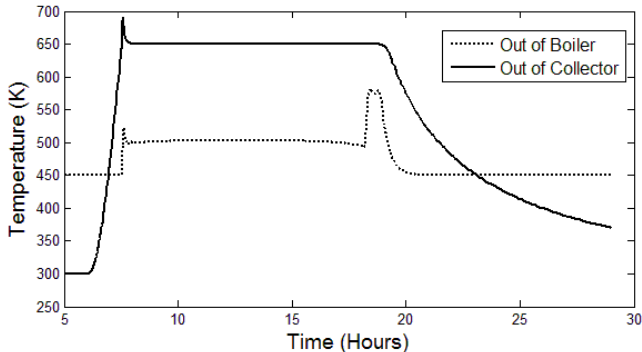


Figure 7: The collector outlet temperature and the boiler outlet temperature of the HTF for a system with no storage.

For a CSP system with no thermal storage, a control scheme designed to maintain a constant power output is not feasible, because the system can only produce power as it is

available from the sun. With no storage, the system is unable to absorb excess energy when it is available and, as a result, there is no stored energy to draw upon when there is a shortage of solar energy.

##### B. Clear Day: System with Storage

The same collector/boiler system is again considered, now with a thermal energy storage system. This setup makes it possible to control the power output and collector outlet temperature independently. The nominal power output used here is 1 MW. The TES system used is the two-tank-direct system with two 64 m<sup>3</sup> tanks, which results in 8 MWh (or approximately 8 hours) of energy storage, given the nominal operating conditions. A larger collector field (3,000 m<sup>2</sup>) is used in order to take advantage of the storage capacity.

The control scheme employed uses the HTF flow rate through the collector as a manipulated variable to keep the outlet temperature constant using PID control. The HTF flow rate through the boiler is used to keep the power output (or equivalently, the steam generation rate) constant using another PID controller. The results of this simulation are shown in Figures 8-11.

As shown in Figure 8, the power controller keeps the power output constant at its set point. Early in the day, when more solar energy is available than the load requires, the energy is harvested by storing excess hot HTF in the hot storage tank. In Figure 9, all points where the collector flow rate is greater than the boiler flow rate indicate charging of the system. When the opposite is true, the system is discharging. This allows the plant to continue to generate steam at a constant rate for several hours after sunset.

As Figures 9-11 indicate, the system has completely charged at  $t=16.43$  hours. However, because excess solar energy is still available, the system is allowed to “overcharge”. When this happens, the collector outlet temperature controller is disabled. The flow into the hot tank is equal to the flow out of the hot tank because the tank is full. This results in reduced flow rates through the collector field and higher temperatures out of the collector field. Additional energy is then harvested in the form of elevated temperatures. While it is beneficial to store more energy, the elevated temperatures result in larger heat losses from the collector field and thermal storage tanks. Additionally, excessive temperatures can cause damage to equipment or can lead to degradation of the HTF. When this occurs, parts of the solar field must be shut down to prevent high temperatures.

Alternatively, more energy could be harvested by using larger tanks to keep the HTF flow rate through the collector high and the collector outlet temperature low. However, this additional capacity would only be utilized on days when conditions are ideal and the additional storage capacity may not be cost effective. The system, therefore, is sized to obtain an optimal combination of solar field area and storage capacity, based on minimizing the annualized costs of the plant. This analysis is done using average solar radiation data for the plant location.

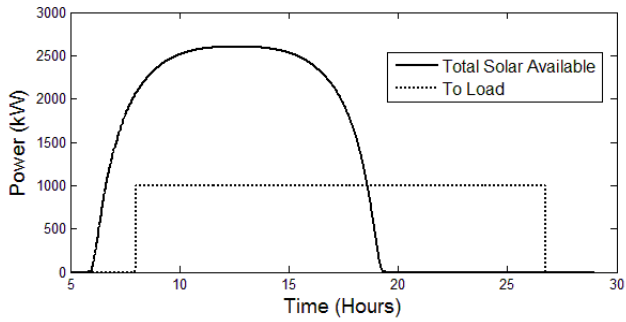


Figure 8: A plot of the total solar energy available and the total power delivered to the load for a system with thermal energy storage.

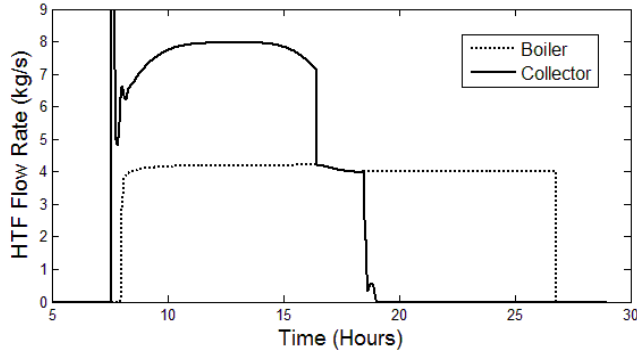


Figure 9: HTF flow rates for a system with thermal energy storage.

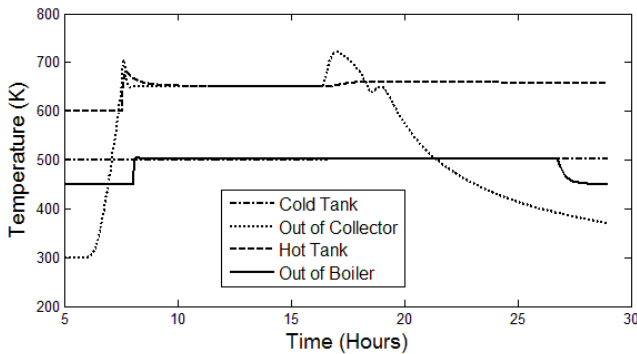


Figure 10: Temperatures for a system with thermal energy storage.

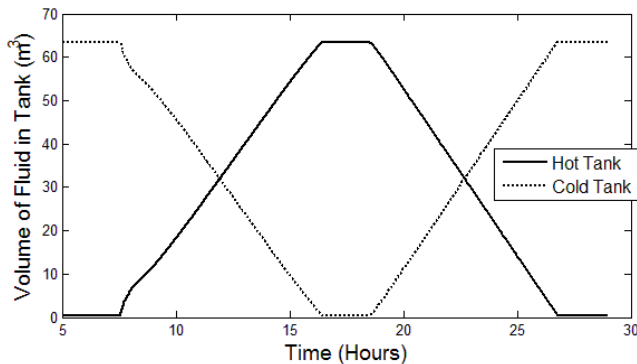


Figure 11: HTF fluid volume in thermal storage tanks.

### C. Cloudy Day: System with No Storage

While parabolic trough collector systems experience several types of disturbances due to changes in ambient conditions (temperature, wind speed, etc.), cloud cover is the most critical disturbance. Cloud cover reduces the amount of solar radiation that is absorbed by the collector field. As a result, a system without thermal energy storage experiences

large interruptions in power output. The cloud factor,  $F_C$ , is modeled using a normally distributed random number,  $R_N$ , generated in 20-minute intervals with mean,  $\mu$ , and variance,  $\Sigma$ , each of which can be adjusted to represent varying degrees of cloud cover.

$$R_N \sim$$

where  $N$  represents a normal-random-number-generating function.  $F_C$  is kept between 0 and 1 by the following:

$$F_C = \begin{cases} 1 & \text{if } R_N > 1 \\ R_N & \text{if } 0 \leq R_N \leq 1 \\ 0 & \text{if } R_N < 0 \end{cases}$$

These results are shown in Figures 12-14. As Figure 12 indicates, intermittent cloud cover causes the power delivered to the load to vary with the available solar radiation.

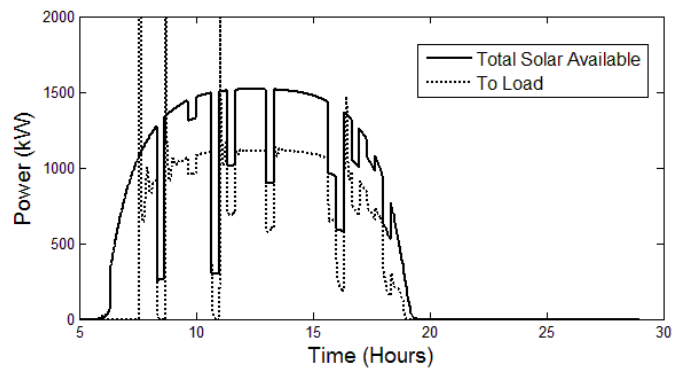


Figure 12: A plot of the total solar energy available and the energy delivered to the load on a partly cloudy day for a system with no storage.

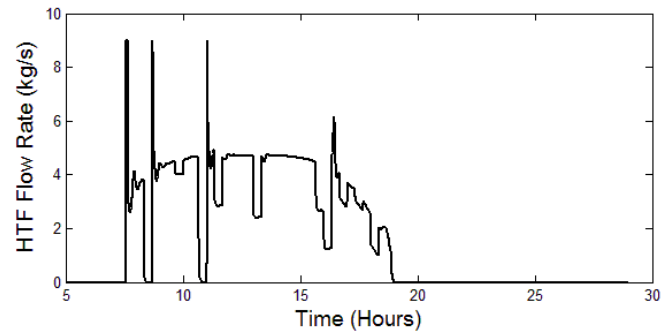


Figure 13: A plot of the HTF flow rate for a system with no thermal storage on a partly cloudy day.

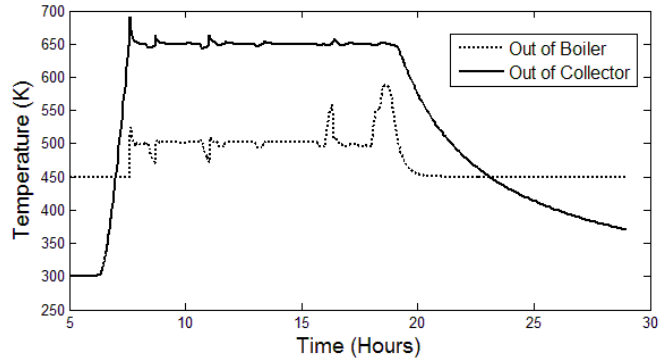


Figure 14: A plot of the HTF exit temperatures from the collector and the boiler for a system with no thermal storage.

#### D. Cloudy Day: System with Storage

The value of thermal energy storage for control of the power output of a concentrating solar system is best seen on days when cloud cover persists. In contrast to the system with no storage, the system with storage maintains a constant power output, despite the fact that solar power is not continuously available. While it is important to control the collector outlet temperature to keep temperatures high enough to deliver heat to the load, it is not necessary to perfectly control this outlet temperature at a constant value. Because the hot storage tank contains a store of energy, the boiler controller can draw upon this to maintain a constant power output. Because less total energy is available on a cloudy day, overcharging of the TES system does not occur in this case. The temperature of the hot storage tank, therefore, remains essentially constant at the collector outlet set point temperature of 650 K.

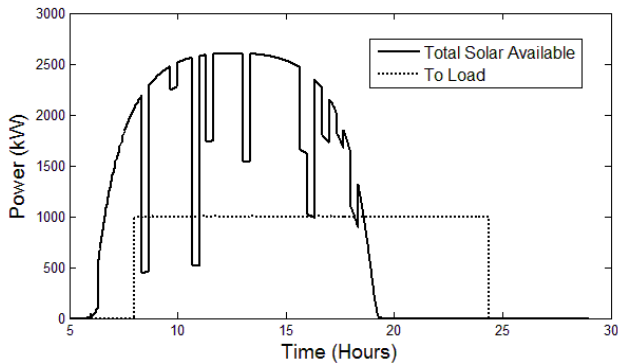


Figure 15: Power available and delivered for a system with thermal storage on a partly cloudy day.

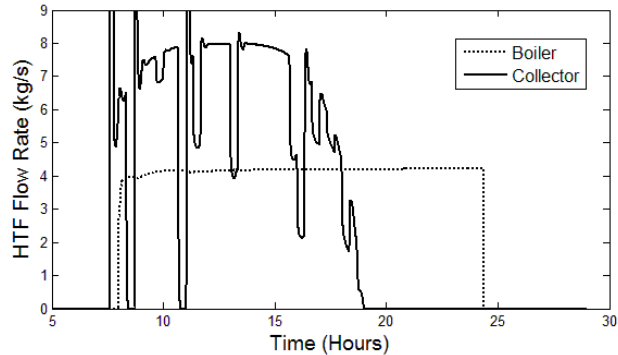


Figure 16: HTF flow rates for a system with storage on a partly cloudy day.

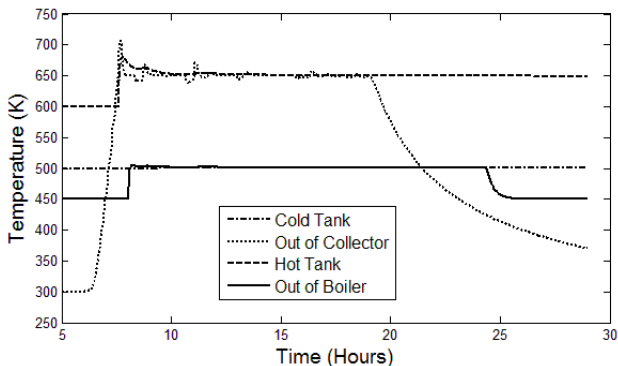


Figure 17: Temperatures for a system with storage on a partly cloudy day.

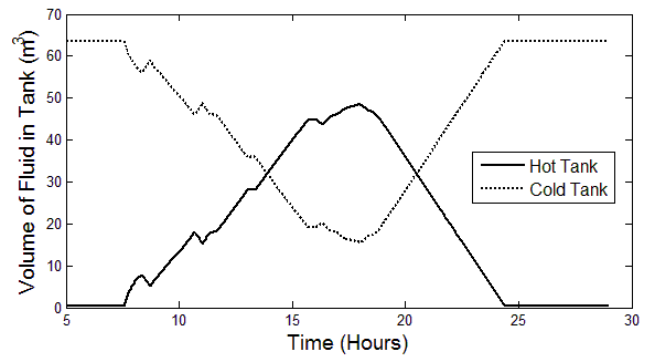


Figure 18: Volume of HTF in the storage tanks for a partly cloudy day.

#### V. CONCLUSION

A summary for each scenario considered is shown in Table 1. The results of these simulations show that by increasing the size of the solar field and adding 8 hours of storage capacity, the solar share (the fraction of energy provided by solar) of the power plant can be increased by over 80% to levels as high as 0.78. With enough storage capacity, it would be possible for a plant to operate 24 hours a day on only solar energy. However, economics dictate that this is not a financially optimal scenario.

	Clear Day: System without Storage	Clear Day: System with Storage	Cloudy Day: System without Storage	Cloudy Day: System with Storage
Supplementary Fossil Fuel Required (MWh)	13.66	5.23	15.19	7.63
Solar Share	0.43	0.78	0.37	0.68

Table 19: A summary of each simulation scenario showing the supplementary fossil fuel required and the solar share.

In addition to increasing the solar share of the power plant by extending the hours of operation, a clear benefit of using storage for solar thermal applications is the ability to maintain a constant power output despite large fluctuations in available sunlight.

#### REFERENCES

- [1] I. Dincer and M.A. Rosen, *Thermal Energy Storage: Systems and Applications*. West Sussex, England: John Wiley & Sons, 2002.
- [2] E.F. Camacho et al., "A survey on control schemes for distributed solar collector fields. Part II: Advanced control approaches," *Solar Energy*, vol. 81, Feb. 2007, pp. 1252-1272.
- [3] A. Gil et al., "State of the art on high temperature thermal energy storage for power generation. Part I-Concepts, materials, and modellization," *Renewable and Sustainable Energy Reviews*, vol. 14, 2010, pp. 31-55.
- [4] S.A. Kalogirou, *Solar Energy Engineering Processes and Systems*. Burlington, MA. Elsevier, 2009.
- [5] M.J. Ahmad and G.N. Tiwari, "Solar Radiation Models-A Review," *International Journal of Energy Research*. Wiley InterScience, www.interscience.wiley.com, 2010.
- [6] J.A. Duffie and W. A. Beckman, *Solar Engineering of Thermal Processes*. 3<sup>rd</sup> Ed. Hoboken, N.J. John Wiley & Sons, 2006.
- [7] D.E. Seborg, T.F. Edgar, and D.A. Mellichamp, *Process Dynamics and Control*. 2<sup>nd</sup> Ed. Hoboken, N.J. John Wiley & Sons, 2004.